

## Bose-Einstein Condensation of Magnons in Atomic Hydrogen Gas

O. Vainio,<sup>1,\*</sup> J. Ahokas,<sup>1</sup> J. Järvinen,<sup>1</sup> L. Lehtonen,<sup>1</sup> S. Novotny,<sup>1</sup> S. Sheludiakov,<sup>1</sup> K.-A. Suominen,<sup>1</sup> S. Vasiliev,<sup>1</sup>  
D. Zvezdov,<sup>1,2</sup> V. V. Khmelenko,<sup>3</sup> and D. M. Lee<sup>3</sup>

<sup>1</sup>*Department of Physics and Astronomy, University of Turku, 20014 Turku, Finland*

<sup>2</sup>*Kazan Federal University, 18 Kremlyovskaya Street, Kazan 420008, Russia*

<sup>3</sup>*Department of Physics and Astronomy and Institute for Quantum Science and Engineering, Texas A&M University, College Station, Texas 77843, USA*

(Received 1 August 2014; published 27 March 2015)

We report on experimental observation of Bose-Einstein condensation (BEC)-like behavior of quantized electron spin waves (magnons) in a dense gas of spin-polarized atomic hydrogen. The magnons are trapped and controlled with inhomogeneous magnetic fields and described by a Schrödinger-like wave equation, in analogy to the BEC experiments with neutral atoms. We have observed the appearance of a sharp feature in the ESR spectrum displaced from the normal spin wave spectrum. We believe that this observation corresponds to a sudden growth of the ground-state population of the magnons and emergence of their spontaneous coherence for hydrogen gas densities exceeding a critical value, dependent on the trapping potential. We interpret the results as a BEC of nonequilibrium magnons which were formed by applying the rf power.

DOI: 10.1103/PhysRevLett.114.125304

PACS numbers: 67.63.Gh, 32.30.Dx, 67.30.hj, 67.85.Jk

In contrast to the Bose-Einstein condensation (BEC) experiments with real particles, e.g., with alkali atoms [1], a condensation of quasiparticles cannot be achieved by lowering the temperature of a thermalized system, but instead a nonequilibrium state is necessary [2]. This overpopulation of quantum states compared to the thermal equilibrium population given by the Planck distribution is achieved by injecting additional quasiparticles to the system externally, i.e., pumping the system. BEC-like behavior, or spontaneous coherence, in systems of coupled oscillators has been predicted by Fröhlich [3] and is often referred to as the Fröhlich coherence. In recent years, a Bose-Einstein-like condensation of quasiparticles has been reported in several distinct systems. These include exciton polaritons [4], triplet states in magnetic insulators [5], magnons in ferromagnets [6] and liquid <sup>3</sup>He [7], and photons in a microcavity [8]. Understanding the properties of quasiparticles is increasingly important due to advancing technologies pushing ever further into the quantum realm.

Quantized electron spin waves (magnons) form a quasiparticle system in a dense quantum gas of ultracold atomic hydrogen [9]. The definition of a quantum gas is that the thermal de Broglie wavelength  $\Lambda_{\text{th}}$  substantially exceeds the scattering length of elastic collisions  $a_s$ . By tuning the magnetic field profile in our experiment, we can modify the magnon-trapping potential. Furthermore, by changing the atomic hydrogen gas density, we are able to modify the spin-exchange interaction strength and thereby the dynamics of the magnons. These two tools together provide unique control of the quasiparticle dynamics and allow the formation of a BEC of magnons similar to that observed in the BEC of neutral atoms [1].

In the present study of dense H gas by electron spin resonance (ESR), we observed a sudden change in the spectrum of the trapped magnons: a sharp and intense peak corresponding to their ground state in the trap grows rapidly after H gas density exceeds a critical value. We believe that this is associated with the emergence of a spontaneous coherence in the system. Based on these two observations, we conclude that the magnons undergo a transition to a BEC when their ground-state energy becomes equal to the chemical potential.

The origin of spin waves in quantum gases is fundamentally different from that in ferromagnets, where the phenomenon is due to the strong *electron* exchange interaction [10]. In quantum gases, weak exchange effects of identical *atoms* lead to a phenomenon known as the identical spin rotation (ISR) effect [11,12]. In the ISR effect, the spins of the interacting atoms rotate around the sum of the spins during binary collisions. The macroscopic propagation of a spin perturbation, the spin wave, is a cumulative result of numerous ISR collisions. The dynamics of the transverse magnetization  $S_+ = S_x + iS_y$  due to the ISR effect is described by the complex spin transport equation, which for strong magnetic fields and small  $S_+$  is [11–13]

$$i \frac{\partial S_+}{\partial t} = D_0 \frac{\varepsilon}{\mu^*} \nabla^2 S_+ + \gamma \delta B_0 S_+, \quad (1)$$

where  $D_0$  is the spin diffusion coefficient in the unpolarized gas,  $\varepsilon = +1$  for bosons and  $-1$  for fermions,  $\gamma$  is the gyromagnetic ratio,  $\delta B_0$  is the deviation of the magnetic field from its average value  $B_0$ , and  $\mu^* \propto \Lambda_{\text{th}}/a_s$  is the spin

wave quality factor. By writing  $m^* = -\hbar\mu^*/2D_0\epsilon$ , Eq. (1) becomes a Schrödinger equation for a particle with an effective mass  $m^*$ . The effective mass of the magnons and the trapped magnon ground-state energies  $\epsilon_0$  both depend on the hydrogen gas density  $n_H$ , since  $D_0 \propto n_H^{-1}$  [13,14]. For our experimental conditions, the effective mass of the magnons is on the order of the free electron mass, making the observation of BEC-like behavior plausible at temperatures substantially higher than those required for the BEC of H atoms [15].

For electron spin waves in hydrogen gas, regions of high magnetic field are minima of the magnetic potential, which is much stronger and of opposite sign than that for nuclear spin waves [14]. Because of weakness of the ISR effect, the influence of the magnetic field inhomogeneities on the dynamics of electron spin waves in hydrogen gas is much stronger than that for ferromagnets.

The experiments are conducted in a high magnetic field of 4.6 T, and therefore the electron and nuclear spin projections  $S$  and  $I$  are good quantum numbers. For the same reason, the induced transverse magnetization  $S_+$  is a small perturbation to the spin polarization. Most of the other spin wave experiments in quantum gases have been conducted in low fields, where the total spin  $F$  is a good quantum number [16,17]. In these experiments, spin self-rephasing and spatial segregation have been observed, which is consistent with the onset of Bose-Einstein condensation. In this work, we report the first observation of spontaneous coherence due to BEC-like behavior of magnons in a quantum gas.

For excitation (pumping) and detection of the spin waves, we use ESR spectroscopy at 129 GHz resonant with the ESR transition from the electron-nuclear polarized hyperfine state [18]. For generating the spin waves, a spatially inhomogeneous excitation is created by an evanescent tail of the rf field [9]. We use both continuous-wave (cw) and pulsed ESR methods. The temperature in our experiments ranges from 200 to 600 mK. Accurate control of the gas density and volume is achieved by a liquid-helium piston operated with a fountain valve, which also provides an independent measurement of the hydrogen gas pressure [9,19,20]. By compressing the gas with this method, we are able to produce hydrogen gas densities from  $10^{16}$  to  $5 \times 10^{18}$  cm $^{-3}$ . The experimental setup is described in more detail in Ref. [19].

The inner walls of the hydrogen gas volume are covered with liquid helium and function as reflective mirrors for the spin waves [14]. In addition, there are magnetic field inhomogeneities inside the sample volume, which in combination with the liquid-helium walls create a potential well for the electron spin waves. We can control the strength and position of these magnetic field deviations with sets of gradient coils outside the sample volume. Additionally, due to the behavior of the liquid-helium piston, we produced two distinctively different magnon trap geometries: one toroidal and another with the shape of a spherical cap [19]. In the toroidal trap,  $n_H$  and  $\epsilon_0$  are lower, and the density of magnon states is higher than in the spherical trap.

In Figs. 1(a) and 1(b), several ESR spectra recorded both below and above the critical hydrogen gas density in both

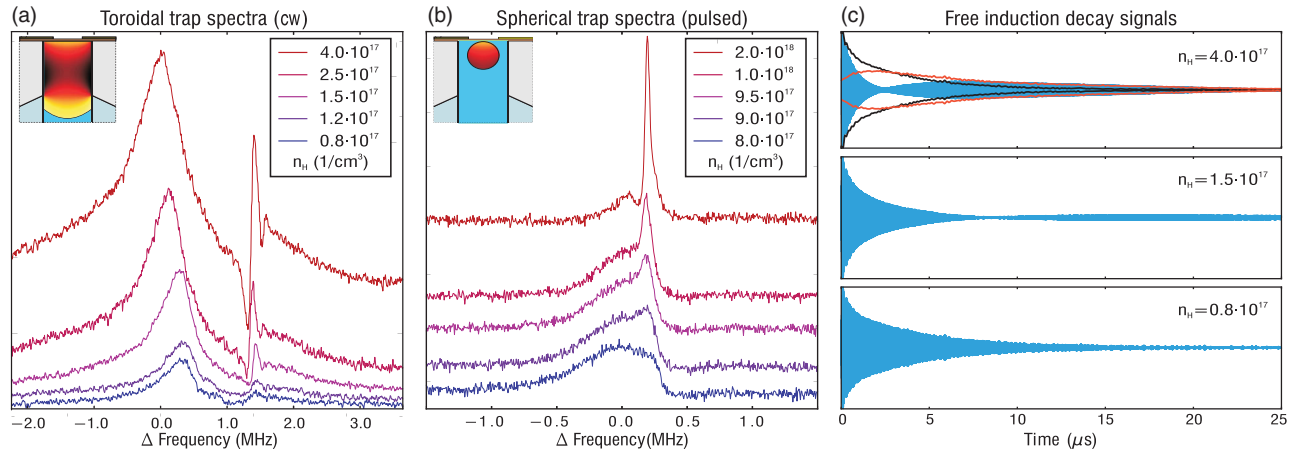


FIG. 1 (color). cw (a) and pulsed (b) ESR spectra with a signal from trapped magnons at five different hydrogen gas densities in the two different trapping geometries (depicted in insets) described in Ref. [19]. In the low density spectra in (a), the left side peak is due to ESR absorption at the rf field maximum, and the right side peak is the signal from the trapped magnons. Because of broadening, the peaks are partially superimposed in the higher density spectra. In (b), only the signal from trapped magnons is visible. In both trapping geometries, the emergence of the spontaneous coherence is visible as a narrow high-amplitude feature. (c) Pulsed ESR (FID) signals below (bottom), above (top), and approximately at the critical hydrogen gas density (middle). In the top panel, the envelopes of the decomposition of the measured signal (blue) into the coherent (red) and incoherent (black) signals is shown. The node in the blue signal is due to destructive interference between coherent and incoherent parts. The continuing growth of the coherent signal amplitude after the end of the excitation pulse is a clear sign of the spontaneity of the coherence. The FIDs are recorded in the toroidal geometry.

trapping geometries are shown. A large number of unresolved spin wave modes trapped in the potential minimum created by magnetic field inhomogeneity are seen as a broad peak on the right side of the ESR spectrum [9]. Above the critical hydrogen gas density, a high-amplitude, narrow-width spectral feature emerges from the trapped magnon peak. Notice the difference in phase between this trapped magnon signal and the main ESR absorption line, which will be discussed later.

We interpret this narrow spectral feature as the emergence of spontaneous coherence resulting from the redistribution of the spin wave modes to the lowest energy mode in the magnetic potential well. Our reasoning is based on the following five arguments: (i) In all our observations, the position of this feature corresponds to the position of the bottom of the magnon potential. (ii) The coherence is established after a short buildup time, not directly at the time of excitation, shown in Fig. 1(c). (iii) We observe critical behavior relative to the hydrogen gas density. (iv) We observe spin transport from higher to lower potential. (v) The coherence has a consistent phase, the offset of which depends on the spatial separation between the trapped magnons and the excitation region.

The coherence is seen in both cw and pulsed ESR spectra, with small variations in appearance due to the differences in the detection techniques. In cw measurements, the magnetic field offset is swept, and the exciting rf field is kept constant. Because of magnetic field inhomogeneities, the spectrum recorded with a cw field sweep is a map of the local absorption (and dispersion) rates inside the sample volume.

In the cw ESR, excitation and detection happen simultaneously and always at the prevailing resonance conditions. Evidence for the coherence in the cw measurements is indicated by the extremely small linewidth associated with the trapped magnons. Another observation confirming the coherent nature of the ground-state signal is its consistent phase difference as compared to the ESR signal from the hydrogen atoms located at the top of the sample volume, in the rf maximum [19]. These atoms produce a broad peak on the left side of the spectra in Fig. 1(a). The phase difference is in accordance with the magnetic field maximum's spatial separation from the main excitation region. For example, an estimated  $l = 0.25$  mm separation between the magnetic field maximum and the rf field ( $\lambda = 2.34$  mm) coupling orifice results in a phase difference  $\Delta\varphi = 4\pi l/\lambda \approx 1.34$ , in good agreement with an observed  $\Delta\varphi$  of approximately  $\pi/2$  [see Fig. 1(a)] [19].

In the pulsed ESR technique, the magnetic field is kept constant, and short pulses of rf excitations are sent to the sample volume. Between the excitation pulses, the free induction decay (FID) signal is recorded. The pulsed spectra in the frequency domain are Fourier transforms of the FID signals, usually averaged over several thousand pulse-detection periods.

In Fig. 1(c), FID signals below, above, and approximately at the critical density are shown. The FID signal with the coherence has a node in its envelope due to destructive interference between the coherent and incoherent signals. In the top panel in Fig. 1(c), the decomposition of the measured signal into coherent and incoherent parts is shown. The amplitude of the coherent part is still growing after the excitation pulse has been switched off. This is a clear sign of spontaneous reorganization of the spins within the sample instead of induced coherence by the excitation pulse. The incoherent signal decays rapidly because of differences in oscillation frequencies of the large number of magnon modes out of which it is composed. The coherent signal, in contrast, originates from a single (ground-state) mode and therefore has a longer decay time. The coherence has been observed in various potentials in two distinct sample gas geometries [19]. Similar signals have also been seen in systems of liquid  $^3\text{He}$  [7] and a quantum gas of  $^{87}\text{Rb}$  [17].

By varying the pulse length and shape, the spectral width of the excitation can be manipulated. This can be used for selective excitation of limited regions of the sample volume. Figure 2 shows two different pulsed ESR spectra resulting from two different locations being selectively excited. An excitation that is resonant at the top of the sample volume, at a distance from the magnon trap bottom, still produces a disproportionately strong signal from the magnon trap bottom (purple curves). In contrast, an excitation resonant at the trap bottom only produces a single narrow-bandwidth high-amplitude spectral peak (green curves). We interpret this as spin transport from higher potential towards the bottom of the spin wave trap.

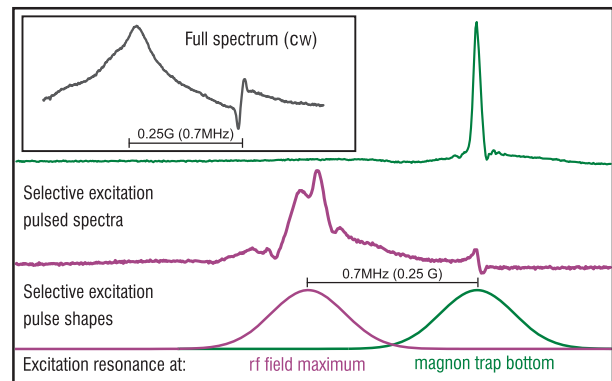


FIG. 2 (color). Spectra measured with selective excitation pulses. Green and magenta curves show selective excitation pulse shapes and the measured spectra, correspondingly. Excitation in resonance with hydrogen atoms located at the rf field maximum (purple curves), spatially separated from the minimum of the magnon potential, still produces a signal from the bottom of the potential. A similar excitation in resonance with the bottom of the potential (green curves) only produces a signal from the potential minimum. The inset shows the cw spectrum.

During hydrogen atom gas compressions, the spectra evolve smoothly until a sudden growth of the high-amplitude coherent signal begins after the critical density has been reached. The observed  $n_{\text{H}}$ -dependent criticality in the formation of the coherence in different potentials follows the behavior of the simulated ground-state energies  $\epsilon_0(n_{\text{H}})$  for trapped magnons. We argue that changes in the ground-state energy, rather than in the chemical potential, will lead to the ground-state overpopulation. In Fig. 3, curves corresponding to critical behavior of the coherent peak amplitudes of trapped magnon signals for three different potentials are plotted against the hydrogen gas density. In the same figure, the simulated behavior of the corresponding ground-state energies is also shown. The ground-state energies corresponding to our experimental conditions have been found by numerically calculating the eigenmodes and frequencies of the magnon modes for several different hydrogen gas densities using Eq. (1). The density dependence of the ground-state energy closely follows the relation  $\epsilon_0 \propto n_{\text{H}}^{-1/2}$ .

As with other quasiparticle systems, the chemical potential is nonzero only under pumping, e.g., while introducing out-of-equilibrium magnons into the system. In particular, the Bose distribution

$$n_k = [e^{(\epsilon_k - \mu)/(k_B T)} - 1]^{-1} \quad (2)$$

is valid only for the quasiparticles while the system is being pumped and the interstate relaxation rate is much faster than the relaxation to the thermal bath. The details of the magnon thermalization are still unknown. We assume that the rate of thermalization is fast enough to establish the distribution given by Eq. (2).

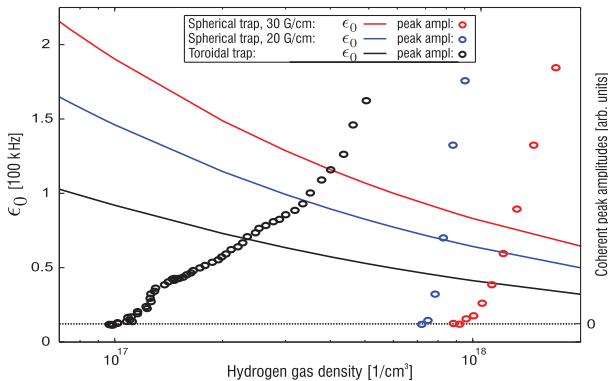


FIG. 3 (color). Ground-state energies for trapped magnons and coherent peak amplitudes of trapped magnon signals vs hydrogen atom density for three different potentials. Solid lines show the simulated ground-state energies  $\epsilon_0$  and circles the detected coherent signal amplitudes vs hydrogen atom density. Black line: Toroidal trap, no applied linear gradient. Blue line: Spherical trap with  $\approx 20$  G/cm gradient. Red line: Spherical trap with  $\approx 30$  G/cm gradient. A clear density- and potential-dependent criticality is observed in the appearance of the coherent signal.

For ISR magnons in atomic hydrogen gas, the magnon pumping rate also depends on the hydrogen gas density as  $I_p \propto W n_{\text{H}}$ , where the probability  $W$  to create a magnon is proportional to the rf power. Consequently, with a fixed rf power, the pumped magnon density is directly proportional to  $n_{\text{H}}$ . The magnon density could also be increased by increasing the rf power, but for spin-polarized hydrogen this approach leads to rapid recombination. In the high temperature limit  $k_B T \gg \epsilon_0$ , well justified in our experiments, the chemical potential  $\mu$  depends on the pumping rate  $I_p$ , temperature  $T$ , ground-state energy  $\epsilon_0$ , and the dissipation rate to the thermal bath  $\tau_1^{-1}$  as [21]

$$\mu = I_p \tau_1 \frac{\epsilon_0^2}{k_B T}. \quad (3)$$

From Eq. (3), it follows that for a given potential and fixed rf power the induced chemical potential does not depend on  $n_{\text{H}}$ , because the density-related changes in the pumping rate compensate for the changes in the ground-state energy. Therefore, the magnon ground-state population  $n_0$  in Eq. (2) depends on density only via the ground-state energy  $\epsilon_0$ .

According to Eq. (2), the divergence of the ground-state population  $n_0$  corresponding to BEC occurs when  $\epsilon_0 = \mu$ , and therefore the equation for the critical pumping rate is

$$I_{pc} \tau_1 = \frac{k_B T}{\epsilon_{0c}}. \quad (4)$$

The observed difference in the critical densities between the potentials is explained by two separate but related factors. First, the ground-state energies for the potentials differ considerably. Second, due to significant differences in the sample gas geometry, the magnon pumping rates  $I_p$  are different [19].

In this work, we have demonstrated that, in a quantum gas of atomic hydrogen, a BEC of magnons can be achieved. The condensed magnons are trapped in a potential well created by a local maximum of the magnetic field and the walls of the experimental cell. The phenomenon is a direct consequence of the Bose statistics, as pumped bosonic quasiparticles preferably accumulate in the ground state [21]. Contrary to the customary behavior of the atomic (real particle) Bose-Einstein condensates [15], the magnons condense at a lower hydrogen gas density in the potential with lower ground-state energy and higher density of states. This follows from the relation  $n_0 \propto (\epsilon_0 - \mu)^{-1}$  ( $\mu \approx \text{const}$ , but  $\epsilon_0 \propto n_{\text{H}}^{-1/2}$ ) for the ground-state population.

The ability to modify the trapping potential by precisely tuning the magnetic field profile opens up many possibilities for further experimentation. An interesting future experiment would be to prepare two tunable coupled traps and study interference effects between two magnon condensates, in analogy to the early experiments with  $^3\text{He}$  [22]

and to the neutral atom interference [23]. Also, the details of the thermalization of magnons in hydrogen gas represent a very interesting topic for a special study.

This work was supported by the Academy of Finland (Grants No. 268745 and No. 260531), the Wihuri Foundation, and NSF Grant No. DMR 1209255. We thank G. Volovik, M. Krusius, V. Eltsov, Yu. Bunkov, and N. Bigelow for useful discussions.

---

\*otarva@utu.fi

- [1] C. J. Pethick and H. Smith, *Bose Einstein Condensation in Dilute Gases*, 2nd ed. (Cambridge University Press, Cambridge, England, 2008).
- [2] V. L. Safonov, *Nonequilibrium Magnons* (Wiley-VCH, New York, 2013).
- [3] H. Fröhlich, *Phys. Lett.* **26A**, 402 (1968).
- [4] J. Kasprzak, M. Richard, S. Kundermann, A. Baas, P. Jeambrun, J. M. J. Keeling, F. M. Marchetti, M. H. Szymaska, R. André, J. L. Staehli, V. Savona, P. B. Littlewood, B. Deveaud, and L. S. Dang, *Nature (London)* **443**, 409 (2006).
- [5] C. Rüegg, N. Cavadini, A. Furrer, H. Güdel, K. Krämer, H. Mutka, A. Wildes, K. Habicht, and P. Vorderwisch, *Nature (London)* **423**, 62 (2003).
- [6] S. O. Demokritov, V. E. Demidov, O. Dzyapko, G. A. Melkov, A. A. Serga, B. Hillebrands, and A. N. Slavin, *Nature (London)* **443**, 430 (2006).
- [7] Y. M. Bunkov and G. E. Volovik, *J. Phys. Condens. Matter* **22**, 164210 (2010).
- [8] J. Klaers, J. Schmitt, F. Vewinger, and M. Weitz, *Nature (London)* **468**, 545 (2010).
- [9] O. Vainio, J. Ahokas, S. Novotny, S. Sheludiyakov, D. Zvezdov, K.-A. Suominen, and S. Vasiliev, *Phys. Rev. Lett.* **108**, 185304 (2012).
- [10] F. Keffer, in *Handbuch der Physik*, edited by H. P. J. Wijn (Springer-Verlag, New York, 1966), Vol. 4/18/2, pp. 1–273.
- [11] C. Lhuillier and F. Laloë, *J. Phys. (Paris)* **43**, 197 (1982).
- [12] C. Lhuillier and F. Laloë, *J. Phys. (Paris)* **43**, 225 (1982).
- [13] L. Lévy and A. Ruckenstein, *Phys. Rev. Lett.* **52**, 1512 (1984).
- [14] N. Bigelow, J. Freed, and D. Lee, *Phys. Rev. Lett.* **63**, 1609 (1989).
- [15] D. Fried, T. Killian, L. Willmann, D. Landhuis, S. Moss, D. Kleppner, and T. Greytak, *Phys. Rev. Lett.* **81**, 3811 (1998).
- [16] H. J. Lewandowski, D. M. Harber, D. L. Whitaker, and E. A. Cornell, *Phys. Rev. Lett.* **88**, 070403 (2002).
- [17] C. Deutsch, F. Ramirez-Martinez, C. Lacroûte, F. Reinhard, T. Schneider, J. Fuchs, F. Piéchon, F. Laloë, J. Reichel, and P. Rosenbusch, *Phys. Rev. Lett.* **105**, 020401 (2010).
- [18] I. Silvera and J. Walraven, in *Progress in Low Temperature Physics*, edited by D. F. Brewer (Elsevier Science, New York, 1986), pp. 139–370.
- [19] See Supplemental Material at <http://link.aps.org/supplemental/10.1103/PhysRevLett.114.125304> for experimental setup details.
- [20] T. Tommila, E. Tjukanov, M. Krusius, and S. Jaakkola, *Phys. Rev. B* **36**, 6837 (1987).
- [21] A. I. Bugrij and V. M. Loktev, *Low Temp. Phys.* **34**, 992 (2008).
- [22] A. S. Borovik-Romanov, Y. M. Bunkov, A. de Vaard, V. V. Dmitriev, V. Makrotsieva, Y. M. Mukharskii, and D. A. Sergatskov, *JETP Lett.* **47**, 478 (1988).
- [23] M. R. Andrews, C. G. Townsend, H.-J. Miesner, D. S. Durfee, D. M. Kurn, and W. Ketterle, *Science* **275**, 637 (1997).